Low bone mineral density is associated with the onset of spontaneous osteonecrosis of the knee

Yasushi Akamatsu[1,2], Naoto Mitsugi[1], Takeshi Hayashi[1], Hideo Kobayashi[1], and Tomoyuki Saito[2]

[1]Department of Orthopaedic Surgery, Yokohama City University Medical Center; [2]Department of Orthopaedic Surgery, Yokohama City University School of Medicine, Yokohama City, Kanagawa, Japan.
Correspondence: akamatsu@yokohama-cu.ac.jp
Submitted 11-06-26. Accepted 12-02-20

Background and purpose **The primary event preceding the onset of symptoms in spontaneous osteonecrosis in the medial femoral condyle (SONK) may be a subchondral insufficiency fracture, which may be associated with underlying low bone mineral density (BMD). However, the pathogenesis of SONK is considered to be multifactorial. Women over 60 years of age tend to have higher incidence of SONK and low BMD. We investigated whether there may be an association between low BMD and SONK in women who are more than 60 years old.**

Methods **We compared the BMD of 26 women with SONK within 3 months after the onset of symptoms to that of 26 control women with medial knee osteoarthritis (OA). All the SONK patients had typical clinical presentations and met specified criteria on MRI. The BMDs measured at the lumbar spine, ipsilateral femoral neck, and knee condyles and the ratios of medial condyle BMD to lateral condyle BMD (medial-lateral ratios) in the femur and tibia were compared between the two groups. The medial-lateral ratios were used as parameters for comparisons of the BMDs at both condyles.**

Results **The mean femoral neck, lateral femoral condyle, and lateral tibial condyle BMDs were between x% and y% lower in the SONK patients than in the OA patients ($p < 0.001$). The mean femoral and tibial medial-lateral ratios were statistically significantly higher in the SONK patients than in the OA patients.**

Interpretation **A proportion of women over 60 years of age have low BMD that progresses rapidly after menopause and can precipitate a microfracture. These findings support the subchondral insufficiency fracture theory for the onset of SONK based on low BMD.**

The pathogenesis of spontaneous osteonecrosis of the medial femoral condyle (SONK) remains unclear, although a primary vascular insult and trauma are widely accepted as common causes. However, the pathogenesis of SONK is probably multifactorial (Zanetti et al. 2003, Robertson et al. 2009). Thus, it may be difficult to explain SONK for all ages and both sexes based on a single factor.

Lotke et al. (1977) first suggested a connection between the onset of SONK and subchondral fracture, which was supported by later reports based on MRI and pathological findings (Lecouvet et al. 1998, Yamamoto and Bullough 2000, Takeda et al. 2008). A subchondral insufficiency fracture may result from underlying osteoporosis (Yamamoto and Bullough 2000). This is consistent with a history of sudden onset of pain without a traumatic event (Ahlbäck et al. 1968). In other cases, obesity (Zanetti et al. 2003), overlying degenerative cartilage changes, meniscal tears (Ahlbäck et al. 1968), and meniscal injury (Robertson et al. 2009) may cause increased mechanical loading in the affected condyle, resulting in subchondral fracture.

One study using high-resolution quantitative computed tomography revealed that osteopenia and osteoporosis could be detected in two-thirds of patients with SONK diagnosed by MRI (Zanetti et al. 2003). These observations suggest that some cases of SONK are induced by subchondral insufficiency fracture that may be associated with an underlying low BMD. The incidence of SONK is more common in women than in men, and most of the patients are over 60 years of age (Lotke et al. 1977). A proportion of women older than 60 years have low BMD that progresses rapidly after menopause. Therefore, investigation of women older than 60 years—who may have a common factor—may be useful in clarifying the pathogenesis of SONK. In addition, because previous papers (Houpt et al. 1983, Mears et al. 2009, Robertson et al. 2009) have suggested the presence of preexisting knee osteoarthritis (OA) in patients with SONK, we compared patients with SONK and patients

DOI 10.3109/17453674.2012.684139

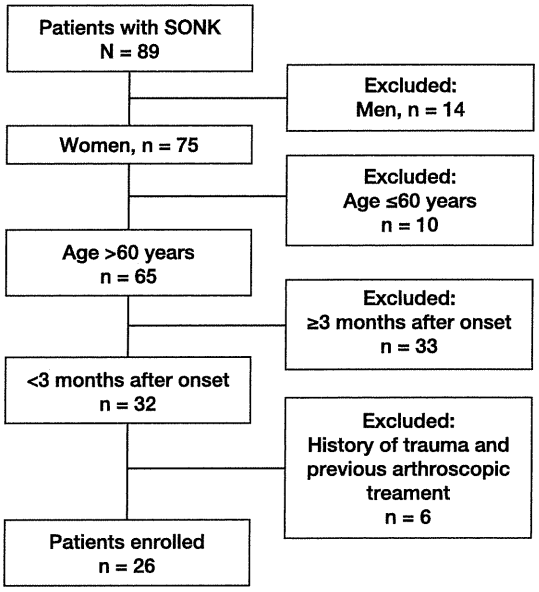

Figure 1. Flow diagram for identifying patients with SONK who were eligible.

with medial knee OA. We assessed the relationship between recent onset of SONK and low BMD at various locations. We also compared the size of lesions by MRI in our SONK patients with those in previous reports.

Patients and methods

Subjects

Between April 2005 and March 2009, we treated 89 consecutive patients with SONK. To target women over 60 years, we excluded 14 men and 10 women who were aged 60 years or less. To minimize the influence of disuse osteoporosis, women with SONK were only enrolled if no more than 3 months had elapsed between the onset of SONK and the time of the BMD measurements. Consequently, of the 65 patients remaining, we excluded 33 women because more than 3 months had elapsed since the onset of symptoms. In addition, we excluded 4 women for having a history of trauma and 2 women for previous arthroscopic treatment. None of the patients with SONK who were included in the study had corticosteroid injections, oral corticosteroid medication, or alcohol abuse. 26 patients remained (Figure 1). All patients were examined by radiography of the knee, knee MRI (Figures 2 and 3), and dual X-ray absorptiometry examinations of the lumbar spine, proximal femur, and knee condyles.

The mean delay between the onset of SONK and its diagnosis based on MRI and BMD measurements was 7 (2–12) weeks. All patients were initially managed nonoperatively. Worsening of knee pain in 15 patients led to surgical treatment mean 17 (6–38) weeks after the initial visit (in 8 patients: high tibial osteotomy; and in 7: a total or unicompartmental knee arthroplasty). Histological sections were obtained from the 15 patients who underwent surgery after a diagnosis of SONK.

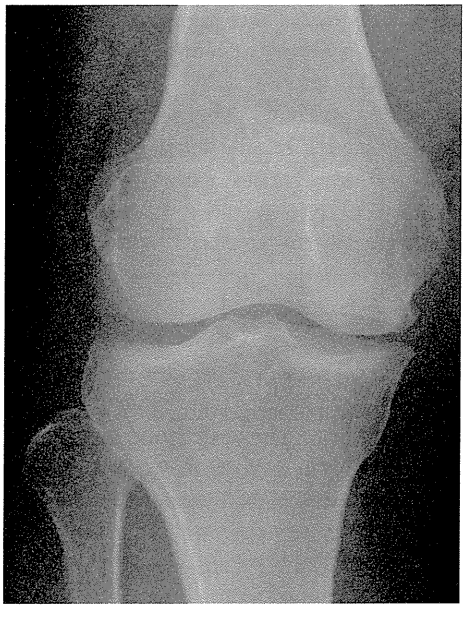

Figure 2. A. An AP radiograph from a 74-year-old woman, who had had sudden onset of right knee pain 7 weeks previously, showing a radiolucent oval lesion in the medial femoral condyle. The patient was classified as being at stage 2 of SONK and Kellgren-Lawrence grade 3.

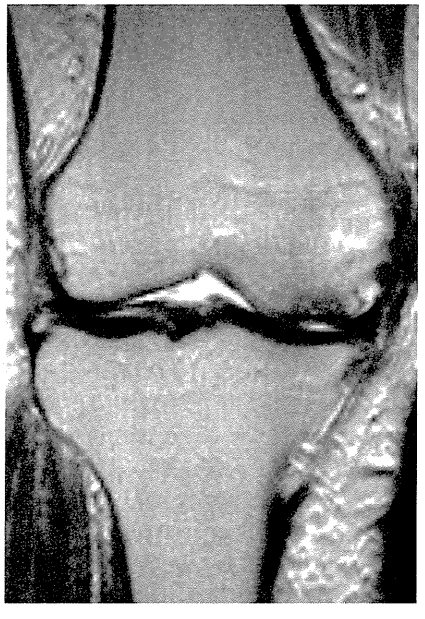

B. A coronal T2-weighted MRI showed an area of low signal intensity.

C. A sagittal T2-weighted MRI with fat suppression showed subchondral changes and extensive bone marrow edema.

Figure 3. A. An AP radiograph from a 65-year-old woman, who had had sudden onset of left knee pain 10 weeks previously, showing no lesions in the medial femoral condyle. The patient was classified as being at stage 1 of SONK and Kellgren-Lawrence Grade 1.

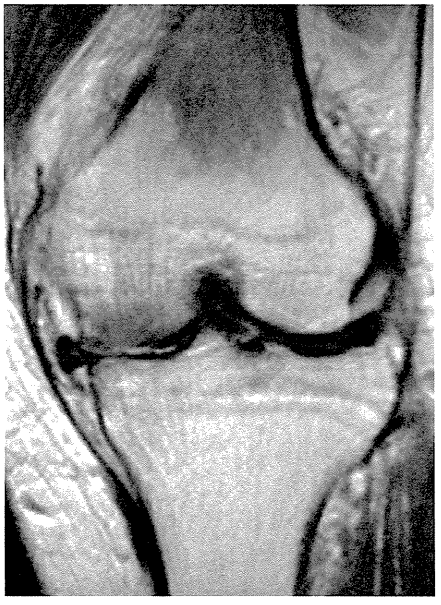

B. A coronal T2-weighted MRI showed an area of low signal intensity.

C. A sagittal T2-weighted MRI with fat suppression showed subchondral changes and bone marrow edema.

The diagnoses of the remaining 11 patients were based on the clinical presentation and imaging findings.

The clinical assessment was primarily based on the criteria established by Ahlbäck et al. (1968) and Lotke et al. (1977), comprising sudden onset of severe pain and localized tenderness over the medial femoral condyle.

Previous studies (Houpt et al. 1983, Mears et al. 2009, Robertson et al. 2009) have suggested the potential of preexisting knee OA in patients with SONK. In patients with medial knee OA, varus alignment can serve as a marker of disease severity or progression (Hunter et al. 2007). Thus, we formed a control group of 26 medial knee OA patients who were matched with respect to age, body mass index, and femorotibial angle (the OA group). These patients were considered to have knee OA if they had Kellgren-Lawrence grades (Kellgren and Lawrence 1957) of 2 or higher, and with a medial joint space narrowing of Ahlbäck grade I (Ahlbäck 1968) or lower. Thus, patients with obliteration of the medial joint space were excluded.

The Knee Society knee, pain, and function scores (Insall et al. 1989) were assigned at the first visit.

The study was approved by our institutional review board (number of approval: 1-10-2005-74), and all patients provided informed consent for participation in the study.

Radiography

AP and lateral knee radiographs were taken with the patients standing. Limb alignment was expressed as the femorotibial angle obtained from the AP knee radiograph. The radiograph was also used to determine the stage of progression of SONK, which was classified into 4 stages (Koshino 1982): stage 1, normal radiographic appearance; stage 2, a radiolucent subchondral oval lesion or flattening of the convexity of the condyle, or both; stage 3, expansion of the radiolucent area surrounded by a sclerotic halo and a calcified plate; stage 4, secondary osteoarthritic changes. 6 knees with stage-1 disease had MRI confirmation and, on follow-up, had stage-2 disease or higher on plain radiographs within 1 year of the onset of disease.

MRI

We used a 1.5-T GE Sigma Scanner (General Electric Medical Systems, Milwaukee, WI). Spin-echo pulse sequences were used exclusively for T1-weighted spin-echo images (repetition time, 610 ms; echo time, 22 ms) and T2-weighted spin-echo images (repetition time, 3,500 ms; echo time, 89 ms). Fat-suppressed images were also obtained. A slice thickness of 3 mm was chosen. The MRI diagnostic criteria for SONK included a discrete low-intensity area on the T1-weighted image and a corresponding low-intensity area with a surrounding high-intensity area, suggestive of bone marrow edema, on the T2-weighted and fat-suppressed images of the medial femoral condyle (Lotke and Ecker 1988, Lecouvet et al. 1998).

All the SONK patients had findings in the weight-bearing area on MRI. In addition, we used the necrotic angle to measure the size of the epiphyseal lesion on MRI (Mont et al. 2000). The arcs of involvement of the subchondral lesion were measured using the center of the radius of the lesion, as measured from the epiphyseal scar in the sagittal and coro-

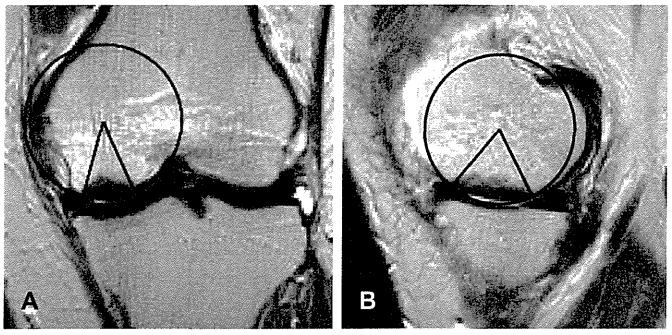

Figure 4. The necrotic angle (Mont et al. 2000) was measure in the sagittal plane (A) and the coronal plane (B). The 2 angles were summed to give the combined necrotic angle. In this case, the combined necrotic angle was 108° (40° + 68°).

nal planes (Figure 4). The 2 angles were summed to give the combined necrotic angle, which was used to assess the total lesions. Lesions of 150° or less were categorized as small, lesions of 151–249° were categorized as medium, and lesions of 250° or more were categorized as large.

BMD

We measured the BMD values at L2-L4 in the lumbar spine, the femoral neck, and the knee condyles using a QDR-4500 bone densitometer (Hologic Inc., Bedford, MA). We found no evidence of ipsilateral femoral neck BMD loss compared with the contralateral femoral neck BMD in either the SONK group or the OA group ($p = 0.9$ and $p = 0.4$, respectively). The BMD measurements for the knee condyles were performed with the patient in the supine position on the scanning table, with the knee flexed at an angle of 20° and the axis of the tibia parallel to the scanning table. In the tibial condyles, 5 square regions of interest were marked under a line on the proximal tibia. The medial tibial condyle BMDs in 2 medial square regions of interest and the lateral tibial condyle BMDs in 2 lateral square regions of interest were calculated for the tibia (Figure 5). In addition, we calculated the lateral and medial femoral condyle BMDs in square regions of interest of the same size as those on the proximal tibia marked on the femoral condyles. The ratios of the medial condyle BMD to the lateral condyle BMD (medial-lateral ratios) in the femur and tibia were used as parameters for comparisons of the BMDs at both condyles. Previous data have shown that this method is reliable (Akamatsu et al. 1997).

The patients were categorized according to the WHO definition (1994). A T-score of more than −1 was defined as normal, osteopenia was defined as a T-score of −1 to −2.49, and osteoporosis was defined as a T-score of −2.5 or less. In addition, low BMD was defined as a T score of −1 or less, which meant the sum of osteopenia and osteoporosis.

Statistics

Data were expressed as the mean with 95% confidence interval (CI). Values were checked for normal distribution with the Shapiro-Wilk test. Differences between the groups were determined by Student's t-test for continuous variables with normal distribution (age, height, weight, femorotibial angle, lumbar spine BMD, femoral neck BMD, lateral femoral condyle BMD, medial tibial condyle BMD, lateral tibial condyle BMD, and medial-lateral ratios); the Mann-Whitney test was used for continuous variables without normal distribution (BMI, Knee Society scores, and medial femoral condyle BMD); and the Pearson chi-square test (low BMD or normal based on the T scores at the lumbar spine) or Fisher's exact probability test (low BMD or normal based on the T-scores at the femoral neck) was used for nominal variables. SPSS software version 17 was used for the statistical analyses. Values of $p < 0.05$ were considered significant. We performed a priori power analysis to ensure that the study was not underpowered. Since were no similar previous studies, we compared the BMDs between the two groups using a Cohen's large effect size of 0.8 and a significance level of 0.05. We found that 80% power corresponded to a sample size of 26 subjects per group.

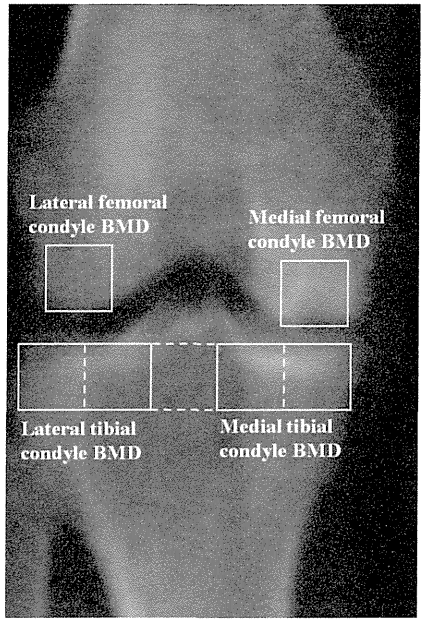

Figure 5. An AP dual X-ray absorptiometry image of the right knee of a 74-year-old woman 7 weeks after the onset of pain (the same patient as in Figure 2) showing a necrotic lesion surrounded by a sclerotic area in the medial femoral condyle. In the tibial condyles, five square regions of interest were marked on the frontal view. A line extending to the lateral and medial edges of the proximal tibia was divided into 5 equal lengths and 5 square regions of interest were marked underneath it. The medial tibial condyle BMDs in the 2 medial square regions of interest and the lateral tibial condyle BMDs in the 2 lateral square regions of interest were calculated for the tibia. In addition, the lateral and medial femoral condyle BMDs were calculated in square regions of interest of the same size as those on the tibial condyles located on a line passing through the tips of the medial and lateral condyles, with the midpoints of their distal sides at the points of contact.

Table 1. Patient characteristics. The values are given as mean (95% CI)

Variable	SONK (n = 26)	OA (n = 26)	95% CI for difference	p-value
Age, years	72 (70–74)	71 (68–73)	–1.5 to 4.7	0.3 [a]
Height, cm	150 (147–152)	152 (149–154)	–5.2 to 1.5	0.3 [a]
Weight, kg	55 (52–59)	55 (52–58)	–4.0 to 4.5	0.9 [a]
Body mass index, kg/m^2	25 (23–26)	24 (23–25)		0.4 [b]
Knee Society score, points				
Knee	53 (48–58)	72 (66–78)		< 0.001 [b]
Pain	20 (17–24)	35 (31–39)		< 0.001 [b]
Function	47 (40–53)	77 (68–86)		< 0.001 [b]

[a] Student's t-test.
[b] Mann-Whitney test.

Table 2. Imaging findings

Variable	SONK (n = 26)	OA (n = 26)	95% CI for difference	p-value
Femorotibial angle (°)	180 (179–181)	179 (178–190)	–0.2 to 2.1	0.1 [a]
Kellgren-Lawrence grade (knees)				
Grade 1	5	0		
Grade 2	19	8		
Grade 3–4	2	18		
Radiographic stage (knees)				
Stage 1	7			
Stage 2	19			
Stage 3 to 4	0			
Combined necrotic angle (°)	165 (154–176)			
Lesion size (knees)				
Small	7			
Medium	19			
Large	0			

[a] Student's t-test.

Results

2 of the authors (YA, NM) measured the femorotibial angle on 135 knee radiographs and the interobserver interclass correlation coefficient was 0.996. In addition, the same authors classified the SONK lesions, and the kappa coefficient to determine the interobserver agreement of the radiographic staging was 0.88.

At entry into the study, the mean Knee Society knee, pain, and function scores were higher in the OA group than in the SONK group (Table 1).

All knees with spontaneous osteonecrosis had femorotibial angles of more than 174°; the Kellgren and Lawrence grades were grade 1 in 5 knees, grade 2 in 19 knees, and grade 3 in 2 knees. In the OA group, the Kellgren and Lawrence grades were grade 2 in 8 knees and grades 3–4 in 18 knees. The radiographic stages of SONK at the time of diagnosis were stage 1 in 7 knees and stage 2 in 19 knees. The mean combined necrotic angle of the SONK group was 165°. Small lesions were noted in 7 knees and medium lesions were noted in 19 knees (Table 2).

The mean femoral neck BMD was lower in the SONK group than in the OA group (CI for difference: –0.12 to –0.04; $p < 0.001$). All the knees in the SONK group had low BMDs at the femoral neck, and 20 of 26 knees in the OA group had low BMDs at the femoral neck ($p = 0.02$). However, there was no statistically significant difference in mean lumbar spine BMD between the 2 groups. The mean lateral femoral and tibial condyle BMDs were significantly lower in the SONK group than in the OA group (CI for difference: –0.19 to –0.07, $p < 0.001$; and CI for difference: –0.20 to –0.06, $p < 0.001$, respectively). However, the mean medial femoral and medial tibial condyle BMDs were similar between the two groups. The mean femoral and tibial medial-lateral ratios were significantly higher in the SONK group than in the OA group (CI for difference: 0.17–0.58, $p = 0.001$; and CI for difference: 0.01–0.34, $p = 0.04$, respectively) (Table3).

Discussion

We found that BMD of the femoral neck, lateral femoral condyle, and lateral tibial condyle were significantly lower in the SONK patients than in the OA patients. Also, the femoral and tibial medial-lateral ratios were significantly higher in the SONK patients than in the OA patients. Our findings support the subchondral insufficiency fracture theory for the onset of SONK from low BMD in women > 60 years of age.

The SONK group had a significantly lower BMD at the femoral neck than the OA group, and all the SONK patients had low BMDs at the femoral neck. In addition, similar to the case of the femoral neck, the SONK group had significantly lower BMDs at the lateral femoral and lateral tibial condyles than the OA group. The lateral condyle BMDs represent the BMD of the ipsilateral lower extremity in all of the knee condyles, as we found in a previous study (Akamatsu et al. 2009). These findings therefore suggest that recent onset of SONK has an association with low BMD in women over 60 years. The SONK group had lower BMD values at the femoral neck, but not at the lumbar spine, than the OA group. The hip is less affected by OA with age than the spine. Because lumbar spine osteophytes affect most subjects over 60 years and indicate false higher lumbar spine BMD values, diagnosis of osteoporosis in the elderly should be based on hip BMD (Liu et al. 1997). We therefore evaluated the BMD values at the femoral neck.

Table 3. BMD at various locations and medial-lateral ratios. The values are given as mean (95% CI)

Variable	SONK (n = 26)	OA (n = 26)	95% CI for difference	p-value
Lumbar spine BMD, g/cm^2	0.79 (0.73–0.84)	0.84 (0.79–0.89)	–0.13 to 0.02	0.2 [b]
Based on the T score at the lumbar spine				
Low BMD [a] / Normal BMD (knees)	20 / 6	20 / 6		1.0
Femoral neck BMD, g/cm^2	0.54 (0.51–0.56)	0.62 (0.59–0.65)	–0.12 to –0.04	< 0.001 [b]
Based on the T score at the femoral neck				
Low BMD [a] / Normal BMD (knees)	26 / 0	20 / 6		0.01
Medial femoral condyle BMD, g/cm^2	1.04 (0.96–1.12)	1.02 (0.95–1.09)		1.0 [c]
Lateral femoral condyle BMD, g/cm^2	0.57 (0.53–0.61)	0.70 (0.65–0.75)	–0.19 to –0.07	< 0.001 [b]
Femoral medial-lateral ratio	1.86 (1.69–2.03)	1.48 (1.36–1.60)	0.17 to 0.58	0.001 [b]
Medial tibial condyle BMD, g/cm^2	0.78 (0.69–0.86)	0.82 (0.75–0.89)	–0.15 to 0.04	0.2 [b]
Lateral tibial condyle BMD, g/cm^2	0.52 (0.48–0.57)	0.65 (0.60–0.71)	–0.20 to –0.06	< 0.001 [b]
Tibial medial-lateral ratio	1.45 (1.31–1.59)	1.27 (1.18–1.36)	0.01 to 0.34	0.04 [b]

[a] Low BMD was defined as a T score of –1 or less.
[b] Student's t-test.
[c] Mann-Whitney test.

Abnormal medial-lateral ratio, which is a parameter for comparison of the medial condyle BMD with the lateral condyle BMD, in patients with knee OA is associated with increases in varus deformity (Akamatsu et al. 1997), bone marrow lesions, osteophytes, joint space narrowing, and sclerosis (Lo et al. 2006). We have found study on the comparison in the medial-lateral ratios between the SONK and the OA groups. The higher femoral medial-lateral ratio in the SONK group than in the OA group in our study corresponds to previous scintigraphic findings that the mean medial-lateral ratios of the distal femur plus proximal tibia in the early phase of SONK were higher than the ratios in knee OA (Muheim et al. 1970). We speculate these results show new bone formation accompanying the onset of SONK. We detected bone formation in the medial femoral condyle prior to the radiographic detection of the surrounding sclerotic halo.

Previous papers (Houpt et al. 1983, Mears et al. 2009, Robertson et al. 2009) have suggested the presence of preexisting knee OA in patients with SONK. It is likely that knee OA is common in women older than 60 years, and that most of our SONK patients had knee OA before the onset of osteonecrosis. We found Kellgren-Lawrence grades of 2 or higher in the knees of 21 of the 26 patients with SONK. This finding of preexisting knee OA in our SONK group is similar to published results (Houpt et al. 1983, Mears et al. 2009). Furthermore, overlying degenerative cartilage changes and medial meniscus or meniscal root injury (Ahlbäck et al. 1968, Robertson et al. 2009), which could be degenerative osteoarthritic changes, may weaken the load-bearing capacity (Narváez et al. 2003) and occur with increased loading at the medial femoral condyle, resulting in subchondral fracture. Thus, the pathogenesis of SONK may not only be related to low BMD but also to preexisting knee OA.

The degree of the combined necrotic angle on MRI correlates with the prognosis (Mont et al. 2000, Yates et al. 2007), with one report describing patients who had small combined necrotic angles of 150° or less and who were all clinically recovered at mean 5 months after the onset of disease (Yates et al. 2007). The mean combined necrotic angle in our SONK group was 165°. One reason for this difference may be related to the fact that our SONK patients all had lesions in the weight-bearing area, unlike in the previous study (Yates et al. 2007).

Our study design had several limitations. First, since we limited our study to subjects who presented within 3 months of the onset of clinical symptoms, only a small number of eligible patients were enrolled—and all cases were diagnosed with stage-1 or stage-2 disease using plain radiographs. The unremarkable radiographic changes delayed the diagnosis (Ahlbäck et al. 1968), and it was difficult to compile patients with SONK at the early stage after disease onset. Second, the lower Knee Society function score in the SONK group than in the OA group resulted from restricted activities of walking and climbing or descending stairs because of severe pain. However, we considered that limiting the duration to within 3 months of the onset of symptoms minimized the influence of disuse osteoporosis, because we found no evidence of differences between the bilateral femoral neck BMDs in the SONK group and the OA group at entry into our study. The distinctions between SONK and the osteonecrotic-like lesions found in knee OA using MRI were equivocal (Ahuja and Bullough 1978). Therefore, the criteria of typical clinical presentations (Ahlbäck et al. 1968, Lotke and Ecker 1988) and lesions in the weight-bearing area (Lotke and Ecker 1988) were essential for diagnosis of SONK in our study.

A recent report has indicated that the use of bisphosphonate prevents collapse in osteonecrosis of the femoral head (Lai et al. 2005). Future investigations should consider whether increasing the BMD, including the use of medications for osteoporosis, is an appropriate nonoperative approach to treatment of patients with SONK.

YA: study design, collection and interpretation of data, and statistical analysis. NM: study design and statistical analysis. TH and HK: collection of data. TS: study design and interpretation of data. All authors contributed to writing of the manuscript.

No competing interests declared.

Ahlbäck S. Osteoarthrosis of the knee: a radiographic investigation. Acta Radiol Diagn (Stockh) (Suppl 277) 1968: 7-72.

Ahlbäck S, Bauer G C, Bohne W H. Spontaneous osteonecrosis of the knee. Arthritis Rheum 1968; 11 (6): 705-33.

Ahuja S C, Bullough P G. Osteonecrosis of the knee: a clinicopathological study in twenty-eight patients. J Bone Joint Surg (Am) 1978; 60 (2): 191-7.

Akamatsu Y, Koshino T, Saito T, Wada J. Changes in osteosclerosis of the osteoarthritic knee after high tibial osteotomy. Clin Orthop 1997; (334): 207-14.

Akamatsu Y, Mitsugi N, Taki N, Takeuchi R, Saito T. Relationship between low bone mineral density and varus deformity in postmenopausal women with knee osteoarthritis. J Rheum 2009; 36 (3): 592-7.

Houpt J B, Pritzker K P, Alpert B, Greyson N D, Gross A E. Natural history of spontaneous osteonecrosis of the knee (SONK): a review. Semin Arthritis Rheum 1983; 13 (2): 212-27.

Hunter D J, Niu J, Felson D T, Harvey W F, Gross K D, McCree P, Aliabadi P, Sack B, Zhang Y. Knee alignment does not predict incident osteoarthritis: the Framingham Osteoarthritis Study. Arthritis Rheum 2007; 56 (4): 1212-8.

Insall J N, Dorr L D, Scott R D, Scott W N. Rationale of the Knee Society clinical rating system. Clin Orthop 1989; (248): 13-4.

Kellgren J H, Lawrence J S. Radiological assessment of osteo-arthrosis. Ann Rheum Dis 1957; 16 (4): 494-502.

Koshino T. The treatment of spontaneous osteonecrosis of the knee by high tibial osteotomy with and without bone-grafting or drilling of the lesion. J Bone Joint Surg (Am) 1982; 64 (1): 47-58.

Lai K A, Shen W J, Yang C Y, Shao C J, Hsu J T, Lin R M. The use of alendonate to prevent early collapse of the femoral head in patients with nontraumatic osteonecrosis. J Bone Joint Surg (Am) 2005; 87 (10): 2155-9.

Lecouvet F E, van de Berg B C, Maldague B E, Lebon C J, Jamart J, Saleh M, Noël H, Malghem J. Early irreversible osteonecrosis versus transient lesions of the femoral condyles: prognostic value of subchondral bone and marrow changes on MR imaging. Am J Roentgenol 1998; 170 (1): 71-7.

Liu G, Peacock M, Eilam O, Dorulla G, Braunstein E, Johnston C C. Effect of osteoarthritis in the lumbar spine and hip on bone mineral density and diagnosis of osteoporosis in elderly men and women. Osteoporos Int 1997; 7 (6): 564-9.

Lo G H, Zhang Y, McLennan C, Niu J, Kiel D P, McLean R R, Aliabadi P, Felson D T, Hunter D J. The ratio of medial to lateral tibial plateau bone mineral density and compartment-specific tibiofemoral osteoarthritis. Osteoarthritis Cartilage 2006; 14 (10): 984-90.

Lotke P A, Ecker M L. Osteonecrosis of the knee. J Bone Joint Surg (Am) 1988; 70 (3): 470-3.

Lotke P A, Ecker M L, Alavi A. Painful knees in older patients: radionuclide diagnosis of possible osteonecrosis with spontaneous resolution. J Bone Joint Surg (Am) 1977; 59 (5): 617-21.

Mears S C, McCarthy E F, Jones L C, Hungerford D S, Mont M A. Characterization and pathological characteristics of spontaneous osteonecrosis of the knee. Iowa Orthop J 2009; 29: 38-42.

Mont M A, Baumgarten K M, Rifai A, Bluemke D A, Jones L C, Hungerford D S. Atraumatic osteonecrosis of the knee. J Bone Joint Surg (Am) 2000; 82 (9): 1279-90.

Muheim G, Bohne W H. Prognosis in spontaneous osteonecrosis of the knee: investigation by radionuclide scintimetry and radiography. J Bone Joint Surg (Br) 1970; 52 (4): 605-12.

Narváez J A, Narváez J, De Lama E, Sánchez A. Spontaneous osteonecrosis of the knee associated with tibial plateau and femoral condyle insufficiency stress fracture. Eur Radiol 2003; 13 (8): 1843-8.

Robertson D D, Armfield D R, Towers J D, Irrgang J J, Maloney W J, Harner C D. Meniscal root injury and spontaneous osteonecrosis of the knee: an observation. J Bone Joint Surg (Br) 2009; 91 (2): 190-5.

Takeda M, Higuchi H, Kimura M, Kobayashi Y, Terauchi M, Takagishi K. Spontaneous osteonecrosis of the knee: histopathological differences between early and progressive cases. J Bone Joint Surg (Br) 2008; 90 (3): 324-9.

Yamamoto T, Bullough P G. Spontaneous osteonecrosis of the knee: the result of subchondral insufficiency fracture. J Bone Joint Surg (Am) 2000; 82 (6): 858-66.

Yates P J, Calder J D, Stranks G J, Conn K S, Peppercorn D, Thomas N P. Early MRI diagnosis and non-surgical management of spontaneous osteonecrosis of the knee. Knee 2007; 14 (2): 112-6.

Zanetti M, Romero J, Dambacher M A, Hodler J. Osteonecrosis diagnosed on MR images of the knee: relationship to reduced bone mineral density determined by high resolution peripheral quantitative CT. Acta Radiol 2003; 44 (5): 525-31.

Inflamm. Res. (2012) 61:1093–1100
DOI 10.1007/s00011-012-0500-4

Inflammation Research

ORIGINAL RESEARCH PAPER

Cyclic compression-induced p38 activation and subsequent MMP13 expression requires Rho/ROCK activity in bovine cartilage explants

Koichi Nakagawa · Takeshi Teramura · Toshiyuki Takehara · Yuta Onodera · Chiaki Hamanishi · Masao Akagi · Kanji Fukuda

Received: 21 December 2011 / Revised: 23 May 2012 / Accepted: 25 May 2012 / Published online: 12 June 2012

Abstract
Objective Excessive mechanical stress on the cartilage causes the degradation of the matrix, leading to the osteoarthritis (OA). Matrix metalloproteinases 13 (MMP13) is a major catalytic enzyme in OA and p38 plays an important role in its induction. However, precise pathway inducing p38 activation has not been elucidated. We hypothesized here that the small GTPase Rho and its effector ROCK might function in upper part of the mechanical stress-induced matrix degeneration pathway.
Methods Bovine metacarpal phalangeal articular cartilage explants were loaded with 1 MPa dynamic compression for 6 h with or without a ROCK specific inhibitor Y27632 or/and a p38 specific inhibitor SB202190. Then p38 phosphorylation and MMP13 expression were assessed by western blot or/and quantitative RT-PCR. Rho-activity was measured by pull-down assay using glutathione S-transferase fusion protein of Rho binding domain.
Results Cyclic compression caused Rho activation, p38 phosphorylation and MMP13 expression. Both Y27632 and SB202190 were found to block the mechanical stress-enhanced p38 phosphorylation and subsequent MMP13 expression.
Conclusions The present results show that p38 phosphorylation and MMP13 expression are regulated by Rho/ROCK activation, and support the potential novel pathway that Rho/ROCK is in the upper part of the mechanical stress-induced matrix degeneration cascade in cartilage comprised of p38 and MMP13.

Keywords Mechanical stress · Osteoarthritis · Matrix metalloproteinase · Cartilage · Rho/ROCK

Responsible Editor: John Di Battista.

Electronic supplementary material The online version of this article (doi:10.1007/s00011-012-0500-4) contains supplementary material, which is available to authorized users.

K. Nakagawa · C. Hamanishi · M. Akagi · K. Fukuda
Department of Orthopaedic Surgery,
Kinki University Faculty of Medicine, Osaka, Japan

T. Teramura (✉) · T. Takehara · Y. Onodera · K. Fukuda
Division of Cell Biology for Regenerative Medicine,
Institute of Advanced Clinical Medicine, Kinki University
Faculty of Medicine, 377-2 Ohno-higashi, Osaka-sayama,
Osaka 5898511, Japan
e-mail: teramura@med.kindai.ac.jp

K. Fukuda
Department of Rehabilitation Medicine,
Kinki University Faculty of Medicine, Osaka, Japan

Introduction

Alterations of the pattern of weight loading on the joint and resulting mechanical stresses to the articular cartilage tissue may be an important risk factor for initiation and progression of osteoarthritis (OA). In fact, a variety of factors such as joint instability caused by ligament injury, overuse or obesity can contribute to the alteration of the mechanical environment in the joint, and are now regarded as predisposing factors of OA. [1–6]. In healthy cartilage, chondrocytes mediate matrix remodeling through a balance between the synthesis and degradation of the extracellular matrix components. This process is regulated by cytokines, signaling molecules such as mitogen-activated protein kinases (MAPKs), transcription factors and enzymes, and these factors are influenced by the mechanical environment [2, 7, 8]. Therefore, the identification of precise cascades from mechanical stress through

degradation of the cartilage matrix is urgently needed in promoting therapeutic strategies to prevent or treat OA.

It is well established that matrix metalloproteinases (MMPs) accelerate chondrocyte-mediated matrix degradation. Accumulation of MMPs in the synovial fluids due to joint injury has been considered to play an important role in the progression of OA. There are many MMPs involved in cartilage degradation. MMP13 has been considered as the major enzyme involved in OA cartilage erosion [9, 10]. Recent observations indicate that p38 is a major signaling molecule in the induction of MMP13 [11–13]. However, detailed mechanisms regulated by the p38 activity with the mechanical stresses have not been clarified. In other cell types, such as cardiomyocytes, it has been reported that small GTPase Rho could be activated by mechanical forces [14]. The Rho family of small GTP-binding proteins comprises a group of signaling molecules that are activated by a variety of biologically active substances while the GTP-bound form of Rho activates ROCK by binding to the Rho-binding domain (RBD) in ROCK. The ROCK regulates a wide range of biological processes, including reorganization of the cytoskeleton, transcriptional regulation, cell motility, mitogenesis and apoptosis [15, 16]. It has also been suggested that some major signaling molecules in cell physiology including p38 [17, 18] exists as down-stream of the Rho/ROCK signaling cascades.

Here, we focused small GTPase Rho and its effector ROCK as a primary transducer of mechanical stress. Our hypothesis is that Rho/ROCK activity is essential in the mechanical stress-induced p38 activation and MMP13 expression. To determine above hypothesis, we applied cyclic compression on bovine cartilage explants and observed Rho activity, p38 and MMP13 expressions.

Materials and methods

Preparation of the bovine cartilage explant and compression experiment

Full thickness explants of articular cartilage (5 mm diameter) were harvested from the condylar ridge of the metacarpophalangeal joints of freshly slaughtered calves about 10 months of age, which were donated from the local slaughterhouse. The explants were cultured in αMEM (Invitrogen, Carlsbad, CA, USA) with 10 % heat inactivated FCS, and 1 % penicillin/streptomycin (Invitrogen). All compression experiments were performed after allowing explants to equilibrate in culture for 72 h after harvest as previously reported [19]. The test and control explants were removed from adjacent sites on the joint surfaces and paired at harvest to minimize the site-dependent variations. For each experiment, the explants were placed into individual compression wells in 1 ml of culture medium. Prior to the compression treatment, the cartilage explants were precultured in serum-free culture medium composed of 0.1 %BSA (Sigma-Aldrich, St. Louis, MO, USA), DMEM/F-12, 1 % insulin-transferrin selenium (Invitrogen), 1 % sodium pyruvate (Invitrogen) and 1 % antibiotic and anti-micotic solution for 24 h to avoid unnecessary evocation of signaling molecules by FCS. We used Y27632 (Wako Pure Chemical Industries, Osaka, Japan) at 30 μM to inhibit Rho-kinase activity and SB202190 (Wako Pure Chemical Industries) at 15 μM to inhibit p38 activity. All experiments were performed at 37 °C and 5 % CO_2, 95 % in air. Compressive loads were applied to individual explants using the Biopress system: the Flexercell Compression Plus System, FX-4000C (Flexcell International, NC, USA). Mechanical loads were applied as a square waveform at 0.5 Hz (1 s on, 1 s off) corresponding to stress magnitudes of 1 MPa for 6 h to induce degenerating reactions as previously reported [20, 21]. All control specimens were cultured in an unloaded state.

Fluorescent microscopic observation of the activated p38 in the compression-treated cartilage

The compression-treated cartilages were placed in Tissue-Tek cryomolds (Sakura Fine Tek, Tokyo, Japan), embedded in Tissue-Tek OCT compound and frozen on dry ice. Cryosectioning was performed on a Leica CM3050S cryomicrotome (Leica Instruments, Houston, TX, USA). Eight micrometer serial sections were adhered to Poly-prep poly-L-lysine coated slides and visualized on a microscope. Then the slides were fixed in Mildform 10 N for 1 h, washed twice with PBS and blocked by Block ace (Dainippon Pharmaceutical, Osaka, Japan) for 1 h. For immunofluorescent observation, the specimens were incubated with 1/200 diluted anti-phospho-p38 (T180/Y182) rabbit monoclonal antibody (Cell Signaling Technology, Inc., MA, USA, #4511) in 4 °C overnight. The specimens were then washed twice with PBS containing 10 % Block-ace, incubated with 1/1,000 diluted FITC-conjugated anti-rabbit IgG bovine secondary antibody (Santa Cruz Biotechnology, Santa Cruz, CA, USA). After twice washing, FITC labeled specimens were stained with 1/1,000 diluted DAPI and observed using a fluorescent microscope (BZ-9000, Keyence, Osaka, Japan).

Western blot analysis

Cartilage explants or cultured chondrocytes were collected, homogenized in SDS buffer (4 % SDS, 125 mM tris–glycine, 10 % 2-mercaptoethanol, 2 % bromophenol blue in 30 % glycerol) and subjected to polyacrylamide gel electrophoresis in the presence of SDS (SDS/PAGE) followed

by electrotransfer onto PVDF membrane (Hybond-P; Amersham Pharmacia Biotech, Buckinghamshire, UK). The blotted membranes were blocked overnight with Block ace and treated with each primary antibody overnight at 4 °C. Antibody incubations and washes were performed in 0.1 %Tween-20 in PBS throughout. Detection was realized by enhanced chemiluminescence with an ECL plus western blotting detection system (Amersham Pharmacia Biotech, Buckinghamshire, UK) and CCD-based chemiluminescent analyzer LAS 4000. Relative expression level of Rho was quantified by normalizing western blot signals to the housekeeping protein GAPDH. Primary antibodies used in this study were as follows: anti-GAPDH mouse monoclonal antibody (Abnova, Taipei, Taiwan, 226-335); anti-phospho-p38 (T180/Y182) rabbit monoclonal antibody (Cell Signaling Technology, Inc., #4511); anti-p38 rabbit polyclonal antibody (Cell Signaling Technology, Inc., #9212); anti-MMP13 sheep polyclonal antibody (AbD Serotec, Oxford, UK, #5980-1311).

Rho activity analysis

For Rho GTPase analysis, we performed GST pull-down of activated Rho proteins using Active Rho Pull-Down and Detection Kit (Pierce Biotechnology, IL, USA).

Briefly, explants were homogenized by handy-type homogenizer (Multipro 395; Dremel Corporation, WI, USA) in Lysis buffer. Cultured chondrocytes were washed twice with ice-cold PBS and lysed by Lysis buffer. Then the lysates were centrifuged and the supernatants were incubated with affinity gel-bound GST-Rhotekin RBD fusion protein that specifically binds GTP-Rho, and affinity purification was performed with glutathione agarose resin. Total cell lysate or pull-down material was resolved by 10 % SDS-PAGE, followed by immunoblotting with anti-Rho rabbit polyclonal antibody (Thermo Scientific Inc., MA, USA).

Primary culture of the bovine articular chondrocyte and Rho activation by lysophosphatidic acid (LPA) treatment

Chondrocytes were isolated from the articular cartilage by enzymatic digestion with 2 mg/ml of collagenase (Wako Pure Chemical Industries, Osaka, Japan) for 12 h at 37 °C. After filtration, cells were seeded in culture plates and cultured in 10 % FCS supplemented αMEM. Cells were cultured at 37 °C and 5 % CO_2, 5 % O_2. Prior to exposure of LPA, the bovine primary chondrocytes were precultured in serum-free culture medium composed of 0.1 % BSA (Sigma-Aldrich, St. Louis, MO, USA), DMEM/F12, 1 % insulin-transferrin selenium (Invitrogen), 1 % sodium pyruvate (Invitrogen) and 1 % anti-biotic and anti-micotic solution for 24 h. To induce Rho activation, 5/10/20 μM LPA (BIOMOL International, PA, USA) was added and cultured for 6 h before analysis of the *MMP13* gene expression by quantitative RT-PCR. For inhibition experiment of p38 or ROCK signaling, SB202190 or Y27632 were added at 1/5/15 or 1/10/30 μM at the same time with LPA administration.

RNA extraction, reverse transcription and quantitative RT-PCR (qRT-PCR) analysis

Explants or cultured chondrocytes were treated with TRIzol reagent (Invitrogen) and cDNA was prepared from total RNA using random primers under standard conditions with the High Capacity cDNA reverse transcription kit (Applied Biosystems, Foster City, CA, USA). Quantitative RT-PCR was performed using Perfect real-time SYBR green II (Takara Bio, Inc., Shiga, Japan). PCR amplifications were performed with the Thermal Cycler Dice Real Time PCR System (Takara Bio, Inc.) at 95 °C for 10 s followed by 40 cycles of 95 °C for 5 s, 60 °C for 30 s. To quantify the relative expression of each gene, the Ct (threshold cycle) values were normalized for endogenous reference ($\Delta Ct = Ct_{MMP13} - Ct_{Gapdh\beta}$) and compared with a calibrator, using the ΔΔCt method ($\Delta\Delta Ct = \Delta Ct_{sample} - \Delta Ct_{calibrator}$). Each primer pair used in this study were as follows:

Gapdh forward GTGAAGGTCGGAGTGAACG;
reverse TAAAAGCAGCCCTGGTGAC,
MMP13 forward TCCCTTGATGCCATAACCAGTC;
reverse AACAGCTCTGCTTCAACCTGC.

Statistical analysis of the data

Significant difference was detected by Tukey–Kramer HSD test or Student's *t* test. A *p* value of less than 0.05 was considered significant difference.

Results

Cyclic compression provoked small GTPase Rho activation, p38 phosphorylation and MMP13 expression

First, we determined whether MAPK p38 and its downstream molecule MMP13 could be induced by applying the cyclic compression. Phosphorylated p38 was detected at 0.5, 1, 3 and 6 h. MMP13 expressions were detected after 3 h compression (Fig. 1a). When observed by immunofluorescence with an antibody to the phosphorylated p38,

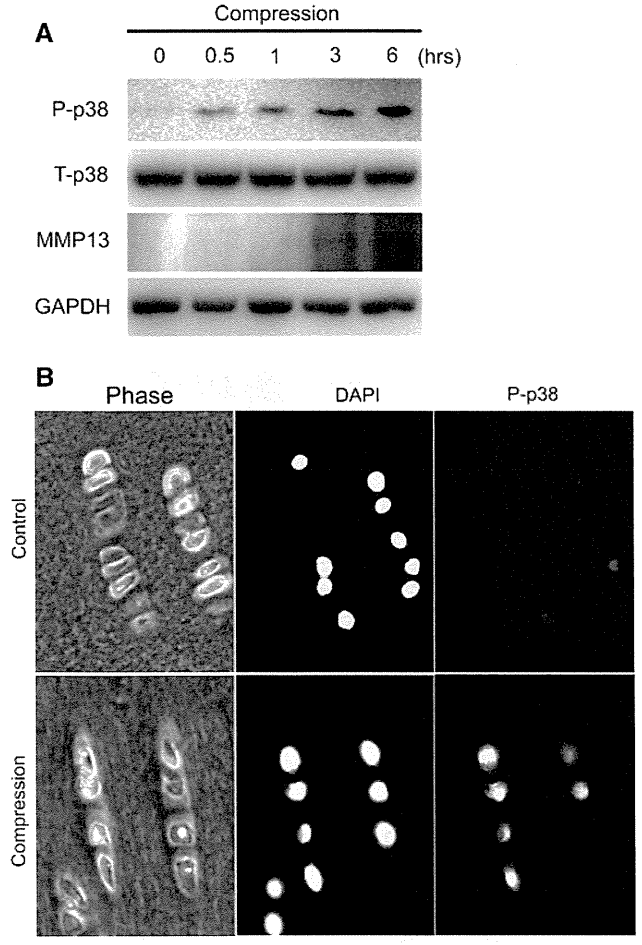

Fig. 1 Effect of compression load to the bovine cartilage explants. **a** Western blot analysis for p38 and MMP13. Phosphorylated p38 (P-p38) was detected in all compressed samples and MMP13 expressions were detected in the samples stimulated for 3 and 6 h. T-p38 means total p38. **b** Immunofluorescent observation of the phosphorylated p38 (P-p38)

clear localization to the nuclei after 6 h continuing compression (Fig. 1b). From these results, we concluded that 6 h compression at the present condition was sufficient to initiate the mechanical stress induced matrix-degrading reaction. Then we examined Rho activity to confirm participation of Rho into the mechanical stress-induced reaction, and found that the Rho activation was initiated at 0.1 h of compression and continued to at least 6 h of compression (Fig. 2a). When the activation was quantified approximately 30 times significant increase of the activated Rho was found after 6 h of compression (Fig. 2b).

Rho activation induced p38 phosphorylation and subsequent MMP13 expression in cultured chondrocyte

Although some major signaling molecules including p38 exist in down-stream of the Rho/ROCK signaling cascades

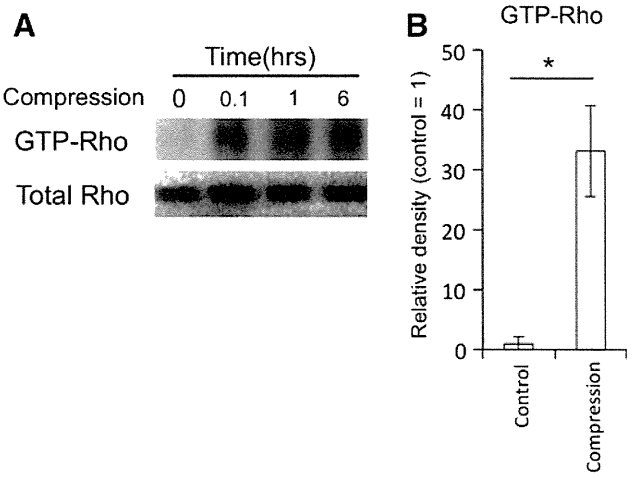

Fig. 2 Rho activation by the cyclic compression stimulation. **a** Activated Rho was detected by GST-pull down method in compression treated samples. **b** Densitometry based quantification of GTP bounded Rho (GTP-Rho). *Asterisk* means significant differences at $p < 0.05$. *Bars* show the mean score of three independent experiments and *bars* depict SD

[17], the effect of Rho/ROCK activation on chondrocyte is still unclear. Then we examined whether Rho activation can bring p38 phosphorylation and subsequent induction of MMP13 expression in chondrocyte by stimulating the bovine primary chondrocyte with LPA, which can chemically invigorate the Rho activity. LPA dramatically activated Rho (Fig. 3a), and caused p38 phosphorylation (Fig. 3b). Furthermore, an increase of MMP13 expression in LPA treated chondrocyte was observed by western blot and qRT-PCR. Administration of SB202190, a selective inhibitor of p38 mitogen-activated protein kinase, into the LPA treated chondrocyte resulted in suppression of the MMP13 gene expression in dose dependent manner (Fig. 3c). On the other hand, adding SB202190 did not lead to diminishing of the phosphorylation status of the p38 as previously reported [22]. Rho-kinase inhibitor Y27632 administration also attenuated the enhancement of the p38 phosphorylation by the LPA treatment when observed by western blot and qRT-PCR (Fig. 3b, c). These results clearly show the possibility that the Rho activation can lead to upregulation of the p38 phosphorylation and following MMP13 expression.

Mechanical stress induced p38 phosphorylation and MMP13 upregulation could be inhibited by administration of ROCK inhibitor

To determine whether p38 phosphorylation and MMP13 expression induced by mechanical stress could be regulated with Rho/ROCK, we applied mechanical stress on the cartilage explant in the presence of SB202190 or/and Y27632. Both SB202190 and Y27632 clearly blocked

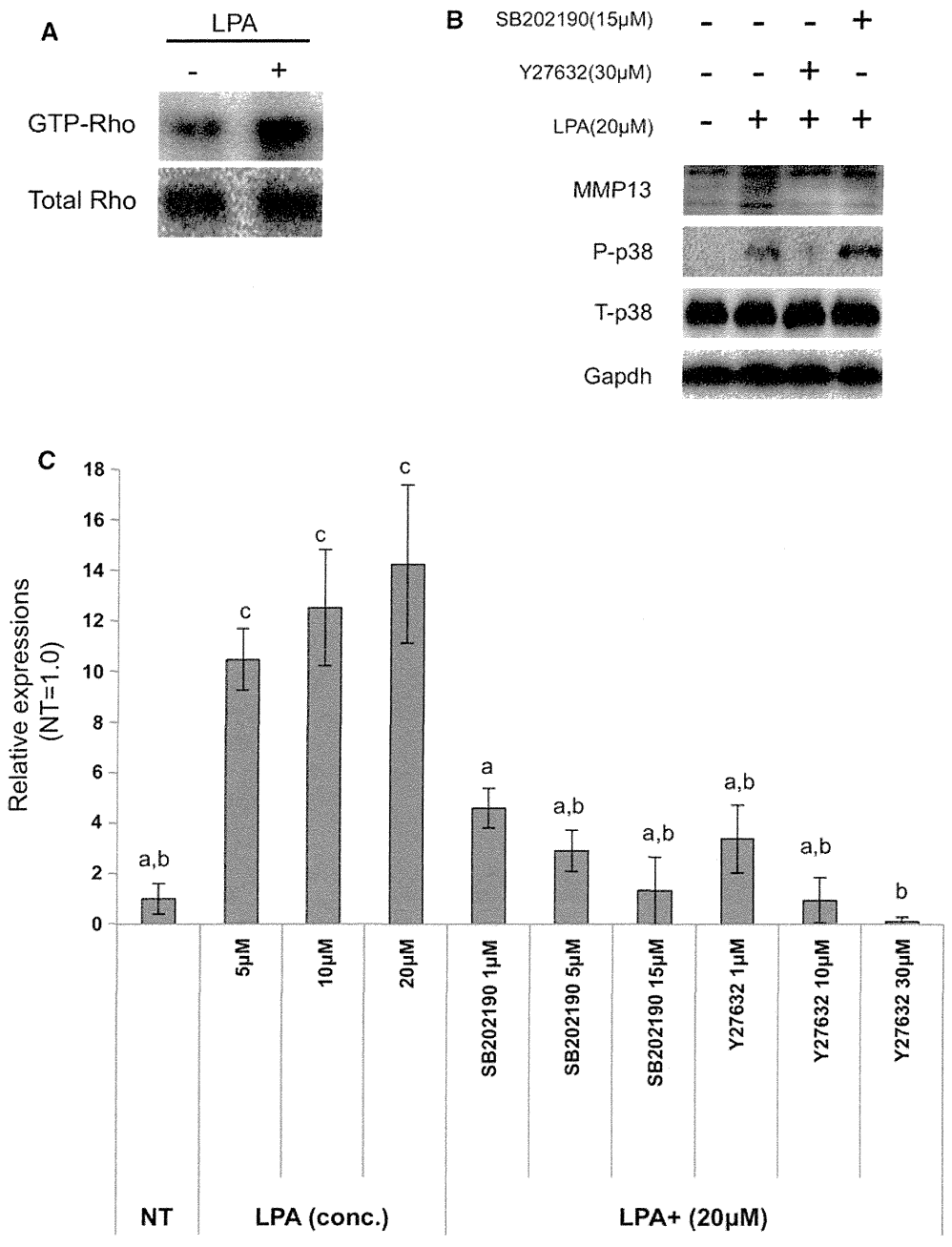

Fig. 3 LPA administration activated Rho and p38, and induced MMP13 expression. **a** Detection of activated Rho by GST-pull down. LPA treatment induced Rho activity. **b** Western blot analysis for p38 and MMP13 of LPA treated primary chondrocyte. **c** qRT-PCR analysis for *MMP13* gene expression. *Different characters* mean significant differences between each experimental group at $p < 0.05$. NT means non-treated control. All experimental groups included the vehicle of SB202190 (DMSO) at same concentration. *Bars* show the mean score of three independent experiments and *bars* depict SD

stress-enhanced p38 phosphorylation and decreased MMP13 quantity. Interestingly, in the present western blot analysis, both activated and inactivated forms of MMP13 were decreased by addition of SB202190 or/and Y27632 (Fig. 4a). qRT-PCR analysis also demonstrated that MMP13 expressions were significantly decreased by the ROCK inhibition (Fig. 4b). At least in the present study, clear differences were observed in the strength of the inhibition effect to the MMP13 expression between the SB202190 and the Y27632. Thus it is possible to assume that the main molecular signaling of mechanical stress-induced matrix degrading reaction leads to MMP13 expression is simply through Rho/ROCK activation and p38 phosphorylation, corresponds to our hypothesis.

Discussion

We considered here that Rho/ROCK is a critical element in the mechanotransduction pathway in the cartilage and possibly involved in the pressure overload-induced matrix degeneration reactions of the cartilage.

Recent studies have demonstrated that p38 can be an effector kinase of mechanotransduction in various types of

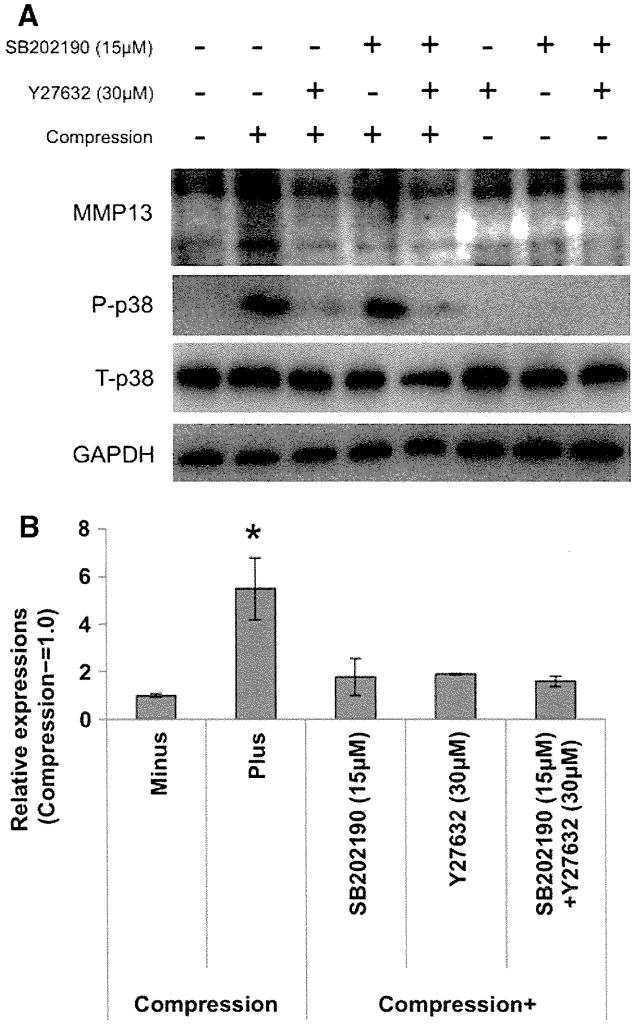

Fig. 4 ROCK inhibition blocked the cyclic compression induced p38 phosphorylation and MMP13 expression. **a** Western blot analysis for p38 and MMP13. **b** qRT-PCR analysis for *MMP13*. Both SB202190 (p38 inhibitor) or/and Y27632 (ROCK inhibitor) supplementation during compression treatment blocked mechanical stress induced *MMP13* expression. *Asterisk* means significant differences at $p < 0.05$. All experimental groups included the vehicle of SB202190 (DMSO) at same concentration. *Bars* show the mean score of three independent experiments and *bars* depict SD

cells. Its function was closely related to chondrocyte matrix metabolism and cell physiology, for example it was shown that p38 could lead to inducing expression of transcription factor Sox9, which regulates the expression of several cartilage-specific matrix components via p38 phosphorylation [23]. Functions of p38 in the cartilage development are important; inhibition of p38 by a dominant-negative (DN) construct, which can interfere with p38 activation results in deficient endochondral bone formation and death shortly after birth. Even if the DN mutation occurs in monoallelic, the heterozygotes represent articular cartilage defects in the knee joints [24]. These facts apparently indicate that p38 is basically essential to articular cartilage. On the other hand, in adult articular tissues, p38 is known to play an important role in inflammatory processes and some evidence suggests that the activity of the p38 can bring about negative effects for the cartilage matrix maintenance [25, 26]. In both OA and rheumatoid arthritis (RA) chondrocytes, it has been shown that p38 is selectively activated to increase MMP13 in response to an inflammatory cytokine IL-1 [13]. Furthermore, Ziegler et al. [27], demonstrated that mechanical stress induced p38 activation could result in MMP13 expression using periodontal ligament cells. Also in the present study, loading of compressive stimulation led to increased p38 phosphorylation and subsequent MMP13 expression. Though the detailed meaning of the mechanical stimulation-reacted evocation of p38 is up for debate, at least these facts suggest that p38 is a major signaling molecule in the induction of MMP13 in articular cartilage, and exploring the upper molecule of p38 is necessary to control the mechanical stress-inducible matrix degeneration reaction of the cartilage. Interestingly, it was reported that the mechanical stimulation-induced p38 phosphorylation is dependent on the α-smooth muscle actin (SMA) filament-dependent pathway [18]. In this work, it was also demonstrated that inhibition of Rho kinase intensely blocked SMA filament assembly, and subsequent mechanical stress-induced p38 activation. Upregulation of Rho activity by mechanical forces has already been demonstrated in various types of cells [14, 28–30] and the direct evocation of p38 phosphorylation by Rho/ROCK has also been reported in cancer cells [17]. Therefore, it is reasonable to consider that small GTPase Rho and its effector kinase ROCK may function in the upper part of the mechanical stress-induced matrix-degrading cascade in cartilage comprised of p38 and MMP13.

Clinically, most important finding from this study may be a fact that the ROCK inhibition actually showed inhibitory effect of p38 and MMP13. To date, specific inhibitors to p38 would be anticipated as novel medicine to RA and OA [31, 32]. On the other hand, since p38 also relates to development and maintenance of chondrocyte specific characteristics, complete interception may result in serious side effects such as defective regeneration of the injured tissues. It is possible that Rho/ROCK inhibition brings about novel alternative strategies for controlling the stress cascades while leading to unfavorable p38 activation and followed by negative reactions of chondrocyte, since it does not directly target p38 and not inhibit p38 activity completely.

To date, some beneficial effects by targeting of ROCK by the specific inhibitor has already determined in patients with cardiovascular diseases such as systemic hypertension [33] and chronic heart failure [34]. However, little is

known about the molecular mechanisms that contribute to increased Rho/ROCK activity or the downstream targets of the Rho/ROCK. The Rho/ROCK functions in chondrocyte are also almost uncovered, but some researchers reported the negative effects of Rho/ROCK on the chondrocyte phenotype. In recent studies it was described that the effects of Rho/ROCK signaling on chondrogenesis appear to be mediated by regulation of both expression and activity of the Sox9 [35]. RhoA, which is the predominant Rho isoform and important possible activator of ROCK, especially inhibits both chondrogenesis and hypertrophic chondrocyte differentiation, while inhibition of RhoA or ROCK promotes chondrocyte maturation. Tew et al. [23] reported that ROCK inhibition by Y27632 increased Sox9 expression in articular chondrocytes, and Novakofski et al. [36], confirmed that inhibition of RhoA by the Rho antagonist C3 transferase increased expression of Sox9 and its target genes collagen II and aggrecan. Importantly, there are reports demonstrating activation of the RhoA in chondrocyte by inflammatory stimulation, such as the cytokine interleukin 1α [36] or transforming growth factor α [37], and the Rho/ROCK signaling is involved in catabolic pathways of chondrocyte homeostasis such as expression of MMP13. Also in our studies, ROCK activation by the overload of the mechanical stress brought about the MMP13 expression. On the other hand, insulin-like growth factor 1, which is an anabolic factor known to plays a key role in the regulation of chondrocyte proteoglycan (PG) metabolism, was reported to repress the RhoA activity [36] contrarily. These results suggest that the Rho/ROCK activity is fundamentally evoked when the cartilage is exposed to the unfavorable extracellular factors such as inflammatory cytokines or destructive mechanical stress, and control of its function directly may lead to inhibit the collagenolytic molecules and to enhance the chondrogenesis.

In contrast, Woods et al. [38] demonstrated that the ROCK inhibition resulted in diminished mRNA levels of the transcriptional co-activators L-Sox5 and Sox6 and a decrease in Sox9 activity subsequently in the three-dimensional micromass cultures of mouse primary limb mesenchymal cells. Interestingly, they previously reported that Rho/ROCK inhibition results in the enhancement of chondrogenesis such as Sox9 activity and collagen II and aggrecan expression in monolayer cultures of a chondrocytic cell line ATDC5 and primary chondrocytes [39], and they concluded that the role of Rho/ROCK was dependent on the cellular context [38]. To date, it was also broadly accepted that the moderate mechanical stimulation enhances matrix synthesis of the chondrocyte [40–42]. From this aspect, if the Rho/ROCK is a common sensor of the wide mechanotransduction, we need to assume the potential risk of complete ROCK inhibition that may leads to diminution of chondrocyte matrix synthesis on the cartilage tissue level. Moreover, the present results were obtained in the model study using bovine normal cartilage tissue with the serum-free condition, thus we think over-interpretation for clinical utility should be avoided. In the actual condition of the OA joint, the injured cartilage may receive multiple stresses adding with the mechanical force in synovial fluid including inflammatory cytokines. Therefore, actual reproducibility in the human OA joint and the realistic value of drugs targeting Rho/ROCK in the treatment of OA needs to be carefully examined in future studies. However, based on some results in vitro and an evidence of pharmacological effects such as pain reduction and chondroprotective effect of a ROCK inhibitor in the rat OA model [43], it is clear that the Rho/ROCK inhibitors are interesting candidates for OA treatment. Detailed elucidation for the function of Rho/ROCK in chondrocyte will directly lead to novel and effective way for prevention and cure of OA.

Acknowledgments We gratefully acknowledge Ms. Naomi Backes Kamimura, Department of Biology-Oriented Science and Technology, Kinki University, for English editing. We also thank Ms. Kanae Shigi and Ms. Naoko Ohoshi for excellent technical assistance.

References

1. Gelber AC, Hochberg MC, Mead LA, Wang NY, Wigley FM, Klag MJ. Joint injury in young adults and risk for subsequent knee and hip osteoarthritis. Ann Intern Med. 2000;133:321–8.
2. Lee JH, Fitzgerald JB, Dimicco MA, Grodzinsky AJ. Mechanical injury of cartilage explants causes specific time-dependent changes in chondrocyte gene expression. Arthritis Rheum. 2005;52:2386–95.
3. Setton LA, Mow VC, Muller FJ, Pita JC, Howell DS. Mechanical properties of canine articular cartilage are significantly altered following transection of the anterior cruciate ligament. J Orthop Res. 1994;12:451–63.
4. Piscoya JL, Fermor B, Kraus VB, Stabler TV, Guilak F. The influence of mechanical compression on the induction of osteoarthritis-related biomarkers in articular cartilage explants. Osteoarthr Cartil. 2005;13:1092–9.
5. Messier SP. Osteoarthritis of the knee and associated factors of age and obesity: effects on gait. Med Sci Sports Exerc. 1994;26:1446–52.
6. Guilak F, Meyer BC, Ratcliffe A, Mow VC. The effects of matrix compression on proteoglycan metabolism in articular cartilage explants. Osteoarthr Cartil. 1994;2:91–101.
7. Sui Y, Lee JH, DiMicco MA, Vanderploeg EJ, Blake SM, Hung HH, et al. Mechanical injury potentiates proteoglycan catabolism induced by interleukin-6 with soluble interleukin-6 receptor and tumor necrosis factor alpha in immature bovine and adult human articular cartilage. Arthritis Rheum. 2009;60:2985–96.
8. Tomiyama T, Fukuda K, Yamazaki K, Hashimoto K, Ueda H, Mori S, et al. Cyclic compression loaded on cartilage explants enhances the production of reactive oxygen species. J Rheumatol. 2007;34:556–62.
9. Moldovan F, Pelletier JP, Hambor J, Cloutier JM, Martel-Pelletier J. Collagenase-3 (matrix metalloprotease 13) is preferentially localized in the deep layer of human arthritic cartilage in situ: in vitro mimicking effect by transforming growth factor beta. Arthritis Rheum. 1997;40:1653–61.

10. van den Berg WB. Osteoarthritis year 2010 in review: pathomechanisms. Osteoarthr Cartil. 2011;19:338–41.
11. Mengshol JA, Vincenti MP, Coon CI, Barchowsky A, Brinckerhoff CE. Interleukin-1 induction of collagenase 3 (matrix metalloproteinase 13) gene expression in chondrocytes requires p38, c-Jun N-terminal kinase, and nuclear factor kappaB: differential regulation of collagenase 1 and collagenase 3. Arthritis Rheum. 2000;43:801–11.
12. Pei Y, Harvey A, Yu XP, Chandrasekhar S, Thirunavukkarasu K. Differential regulation of cytokine-induced MMP-1 and MMP-13 expression by p38 kinase inhibitors in human chondrosarcoma cells: potential role of Runx2 in mediating p38 effects. Osteoarthr Cartil. 2006;14:749–58.
13. Julovi SM, Ito H, Nishitani K, Jackson CJ, Nakamura T. Hyaluronan inhibits matrix metalloproteinase-13 in human arthritic chondrocytes via CD44 and P38. J Orthop Res. 2011;29:258–64.
14. Kawamura S, Miyamoto S, Brown JH. Initiation and transduction of stretch-induced RhoA and Rac1 activation through caveolae: cytoskeletal regulation of ERK translocation. J Biol Chem. 2003;278(33):31111–7. doi:10.1074/jbc.M300725200.
15. Van Aelst L, D'Souza-Schorey C. Rho GTPases and signaling networks. Genes Dev. 1997;11:2295–322.
16. Etienne-Manneville S, Hall A. Rho GTPases in cell biology. Nature. 2002;420:629–35.
17. Ordonez-Moran P, Larriba MJ, Palmer HG, Valero RA, Barbachano A, Dunach M, et al. RhoA-ROCK and p38MAPK-MSK1 mediate vitamin D effects on gene expression, phenotype, and Wnt pathway in colon cancer cells. J Cell Biol. 2008;183:697–710.
18. Wang J, Fan J, Laschinger C, Arora PD, Kapus A, Seth A, et al. Smooth muscle actin determines mechanical force-induced p38 activation. J Biol Chem. 2005;280:7273–84.
19. Miki Y, Teramura T, Tomiyama T, Onodera Y, Matsuoka T, Fukuda K, et al. Hyaluronan reversed proteoglycan synthesis inhibited by mechanical stress: possible involvement of antioxidant effect. Inflamm Res. 2010;59:471–7.
20. De Croos JN, Roughley PJ, Kandel RA. Improved bioengineered cartilage tissue formation following cyclic compression is dependent on upregulation of MT1-MMP. J Orthop Res. 2010;28:921–7.
21. Sanchez C, Pesesse L, Gabay O, Delcour JP, Msika P, Baudouin C, et al. Regulation of subchondral bone osteoblast metabolism by cyclic compression. Arthritis Rheum. 2012;64:1193–203.
22. Dmitrieva NI, Bulavin DV, Fornace AJ Jr, Burg MB. Rapid activation of G2/M checkpoint after hypertonic stress in renal inner medullary epithelial (IME) cells is protective and requires p38 kinase. Proc Natl Acad Sci USA. 2002;99:184–9.
23. Tew SR, Hardingham TE. Regulation of SOX9 mRNA in human articular chondrocytes involving p38 MAPK activation and mRNA stabilization. J Biol Chem. 2006;281:39471–9.
24. Namdari S, Wei L, Moore D, Chen Q. Reduced limb length and worsened osteoarthritis in adult mice after genetic inhibition of p38 MAP kinase activity in cartilage. Arthritis Rheum. 2008;58:3520–9.
25. Sondergaard BC, Schultz N, Madsen SH, Bay-Jensen AC, Kassem M, Karsdal MA. MAPKs are essential upstream signaling pathways in proteolytic cartilage degradation–divergence in pathways leading to aggrecanase and MMP-mediated articular cartilage degradation. Osteoarthr Cartil. 2010;18:279–88.
26. Joos H, Albrecht W, Laufer S, Brenner RE. Influence of p38MAPK inhibition on IL-1beta-stimulated human chondrocytes: a microarray approach. Int J Mol Med. 2009;23:685–93.
27. Ziegler N, Alonso A, Steinberg T, Woodnutt D, Kohl A, Mussig E, et al. Mechano-transduction in periodontal ligament cells identifies activated states of MAP-kinases p42/44 and p38-stress kinase as a mechanism for MMP-13 expression. BMC Cell Biol. 2010;11:10–24.
28. Sarasa-Renedo A, Tunc-Civelek V, Chiquet M. Role of RhoA/ROCK-dependent actin contractility in the induction of tenascin-C by cyclic tensile strain. Exp Cell Res. 2006;312:1361–70.
29. Teramura T, Takehara T, Onodera Y, Nakagawa K, Hamanishi C, Fukuda K. Mechanical stimulation of cyclic tensile strain induces reduction of pluripotent related gene expressions via activation of Rho/ROCK and subsequent decreasing of AKT phosphorylation in human induced pluripotent stem cells. Biochem Biophys Res Commun. 2012;417:836–41.
30. Haudenschild DR, Nguyen B, Chen J, D'Lima DD, Lotz MK. Rho kinase-dependent CCL20 induced by dynamic compression of human chondrocytes. Arthritis Rheum. 2008;58:2735–42.
31. Pargellis C, Regan J. Inhibitors of p38 mitogen-activated protein kinase for the treatment of rheumatoid arthritis. Curr Opin Investig Drugs. 2003;4(5):566–71.
32. Brown KK, Heitmeyer SA, Hookfin EB, Hsieh L, Buchalova M, Taiwo YO, et al. P38 MAP kinase inhibitors as potential therapeutics for the treatment of joint degeneration and pain associated with osteoarthritis. J Inflamm (Lond). 2008;5:22–30.
33. Masumoto A, Hirooka Y, Shimokawa H, Hironaga K, Setoguchi S, Takeshita A. Possible involvement of Rho-kinase in the pathogenesis of hypertension in humans. Hypertension. 2001;38:1307–10.
34. Kishi T, Hirooka Y, Masumoto A, Ito K, Kimura Y, Inokuchi K, et al. Rho-kinase inhibitor improves increased vascular resistance and impaired vasodilation of the forearm in patients with heart failure. Circulation. 2005;111:2741–7.
35. Beier F, Loeser RF. Biology and pathology of Rho GTPase, PI-3 kinase-Akt, and MAP kinase signaling pathways in chondrocytes. J Cell Biochem. 2010;110:573–80.
36. Novakofski K, Boehm A, Fortier L. The small GTPase Rho mediates articular chondrocyte phenotype and morphology in response to interleukin-1alpha and insulin-like growth factor-I. J Orthop Res. 2009;27:58–64.
37. Appleton CT, Usmani SE, Mort JS, Beier F. Rho/ROCK and MEK/ERK activation by transforming growth factor-alpha induces articular cartilage degradation. Lab Invest. 2010;90:20–30.
38. Woods A, Beier F. RhoA/ROCK signaling regulates chondrogenesis in a context-dependent manner. J Biol Chem. 2006;281:13134–40.
39. Woods A, Wang G, Beier F. RhoA/ROCK signaling regulates Sox9 expression and actin organization during chondrogenesis. J Biol Chem. 2005;280:11626–34.
40. Demarteau O, Wendt D, Braccini A, Jakob M, Schafer D, Heberer M, et al. Dynamic compression of cartilage constructs engineered from expanded human articular chondrocytes. Biochem Biophys Res Commun. 2003;310:580–8.
41. Waldman SD, Couto DC, Grynpas MD, Pilliar RM, Kandel RA. A single application of cyclic loading can accelerate matrix deposition and enhance the properties of tissue-engineered cartilage. Osteoarthr Cartil. 2006;14:323–30.
42. Waldman SD, Spiteri CG, Grynpas MD, Pilliar RM, Kandel RA. Long-term intermittent compressive stimulation improves the composition and mechanical properties of tissue-engineered cartilage. Tissue Eng. 2004;10:1323–31.
43. Takeshita N, Yoshimi E, Hatori C, Kumakura F, Seki N, Shimizu Y. Alleviating effects of AS1892802, a Rho kinase inhibitor, on osteoarthritic disorders in rodents. J Pharmacol Sci. 2011;115:481–9.

軟骨細胞分化における miRNA

浅原 弘嗣*

マイクロRNAはノンコーディングRNAの一種であり，20～25塩基ほどの1本鎖RNAである。ターゲットとなる遺伝子のmRNAに結合し，その発現を抑制する機能を持ち，発生，がん，炎症などあらゆる医学・生物学分野において重要な役割を担うことが明らかにされてきている。
本稿では，特に軟骨細胞および関節軟骨組織の発生，および恒常性維持におけるmiRNAの機能を紹介する。

Frontier of epigenome in bone research.

miRNAs in cartilage development.

Department of Systems BioMedicine, Tokyo Medical and Dental University/
Department of Systems BioMedicine, National Research Institute for Child Health and Development, Japan.

Hiroshi Asahara

MicroRNAs (miRs) are ～22 nucleotide non-cording forms of RNA and exhibit tissue or developmental stage specific expression patterns. Recent findings show taht the expression of miR-140, which is specifically expressed in chondrocytes, is reduced in OA chondrocytes. Furthermore, knockdown of miR-140 in mice chondrocytes promotes arthritis in mice. In addition to this, several other miRs have also been shown to play important roles in chondrocytes. Thus, miRs should be critical factors for cartilage development and homeostasis.

はじめに

マイクロRNAはノンコーディングRNAの一種であり，20～25塩基ほどの1本鎖RNAである。ターゲットとなる遺伝子のmRNAに結合し，その発現を抑制する機能を持ち，発生，がん，炎症などあらゆる医学・生物学分野において重要な役割を担うことが明らかにされてきている。

骨・軟骨の発生におけるmiRNAの重要性

通常のmRNAと同様，miRNAはまず数百一数千塩基長のpri-miRNA (primary microRNA) として転写され，さらに，その転写物がいくつかのス

*東京医科歯科大学医歯学総合研究科システム発生・再生医学分野・教授/国立成育医療研究センター研究所・客員研究部長
（あさはら・ひろし）

テップを経て成熟型の機能を持つmiRNAとなる。

核内でまず酵素DroshaとDGCR8により，stem-loop構造の70塩基程度のpre-miRNA (precursor miRNA)に切り出され，さらにそれがExportin-5によって細胞質に運ばれ，DicerおよびTRBP/PACT (transactivation-response element RNA-binding protein/protein activator of the interferon-induced protein kinase)により，20～25塩基のmiRNAを含む2本鎖RNAが生成される。この2本鎖RNAのうちmiRNA側のみがRISC (RNA-induced silencing complex)に結合することで，機能的 (mature) miRNA-RISC複合体となる[1)2)]。

このようなプロセスにおいてDicerは，ほぼすべてのmiRNA生成に不可欠である。しかし，そのノックアウトマウスは胎生期7.5日で死亡するため[3)]，各組織におけるmiRNAの機能研究では，それぞれの組織におけるコンディショナルなDicerノックアウトマウスの解析が行われてきた。

Tabinらは，胎芽全域で特異的にCreを発現するPrx-CreマウスとDicer-Floxマウスを掛け合わせて，四肢特異的なDicerコンディショナルノックアウトマウスを作製し，このマウスの四肢における骨形成は，骨形成パターン自体は保たれていたものの，四肢の短小化がみられることを報告し，軟骨・骨形成においてmiRNAが重要であることを示唆した[4)]。

さらに，内軟骨性骨化初期での軟骨誘導におけるmiRNAの機能研究では，Kronenbergらは，Col2-CreマウスとDicer-Floxマウスを掛け合わせて軟骨特異的なmiRNAノックアウトマウスを作製し[5)]，このマウスには，内軟骨性骨化における軟骨の増殖が減少した結果，肥大軟骨細胞への移行が早まり，骨格の短小化が起きていることを報告した[5)]。このように，軟骨発生分化においてもmiRNAが重要であることが明らかとなった。

軟骨特異的な発現を示すmiRNA

発生期に組織特異的な発現をするmiRNAをシステマティックに解析する目的で，ゼブラフィッシュをモデルにホールマウントインサイチューハイブリダイゼーション (whole mount *in situ* hybridization：WISH)を行った。結果，軟骨に発現を示すものについては，ユビキタスに発現するもの以外に，miR-146，140*，199a，199a*，145の報告がある[6)]。その中でも，140，199a，199a*については，メダカや，ニワトリでも軟骨での発現が報告されている[7)]。特に，miR-140は他の組織では発現が低く，軟骨のみに特異的な発現を示すことが，マウス胎児を用いたWISHによっても報告された[8)]。199a，199a*については，small RNAのライブラリースクリーニングでマウス結合組織での発現が確認されている。miR-140の軟骨における機能については，ゼブラフィッシュを用いた解析においてplatelet-derived growth factor (PDGF)シグナルを介する軟骨分化制御機構が確認された[9)]。

軟骨細胞に特異的に働くmiRNAを同定するため，われわれは，ヒト関節軟骨を用いたmiRNAに対するマイクロアレイ解析を行い，軟骨分化におけるmiR-140のより特異的な発現上昇を確認している[10)]。また，miR-140の発現はMSCsの軟骨分化と正相関し，分化に伴ってSox9，Col2a1のような軟骨分化マーカーと同じ発現増加を示すことも明らかとなった。

miR-140と発生・軟骨ホメオスタシス（図）

miR-140は正常ヒト関節軟骨で高い発現を示

pri-miRNA：primary microRNA，pre-miRNA：precursor miRNA
TRBP/PACT：transactivation-response element RNA-binding protein/protein activator of the interferon-induced protein kinase，RISC：RNA-induced silencing complex，WISH：whole mount *in situ* hybridization
PDGF：platelet-derived growth factor（血小板由来増殖因子）

す一方，変形性関節症（OA）軟骨においてはその発現量は有意に低下しており，IL1-βによる関節軟骨細胞刺激においてもmiR-140の発現は低下することが確認された[10]。これらの結果から，miR-140の発現低下がOAにおける病的な遺伝子発現の誘因となっており，miR-140がOAの病態と関連していることが示唆される[10]。

そのためわれわれは，miR-140ノックアウトマウスとトランスジェニックマウスを作製し，miR-140の機能解析を行った。結果，miR-140ノックアウトマウスは発生異常は認められなかったものの，生後，四肢，体幹，顔面の短小化がみられ，Dicerノックアウトマウスでみられた表現型の一部がmiR-140で説明できることを確認した[11]。

同様の表現型は，われわれとは別のmiR-140ノックアウトマウスでも報告されている[12]。これらの結果から，miR-140が内軟骨性骨成長に不可欠であり，Dnpepを介したbone morphogenetic protein（BMP）シグナル抑制が，その原因の一つとして考えられた。

また，肢芽のマイクロマスカルチャーにおけるmiR-140ノックダウン解析では，BMPシグナルの下流で働くSp1によって軟骨細胞増殖が低下することが報告されており[13]，miR-140が内軟骨性骨成長において，Dnpep，SP1，BMP2といった複数の遺伝子をターゲットとして働いていることが明らかとなった。早期のOAでは関節軟骨の変化のみならず，軟骨下骨の肥厚，柔軟性の

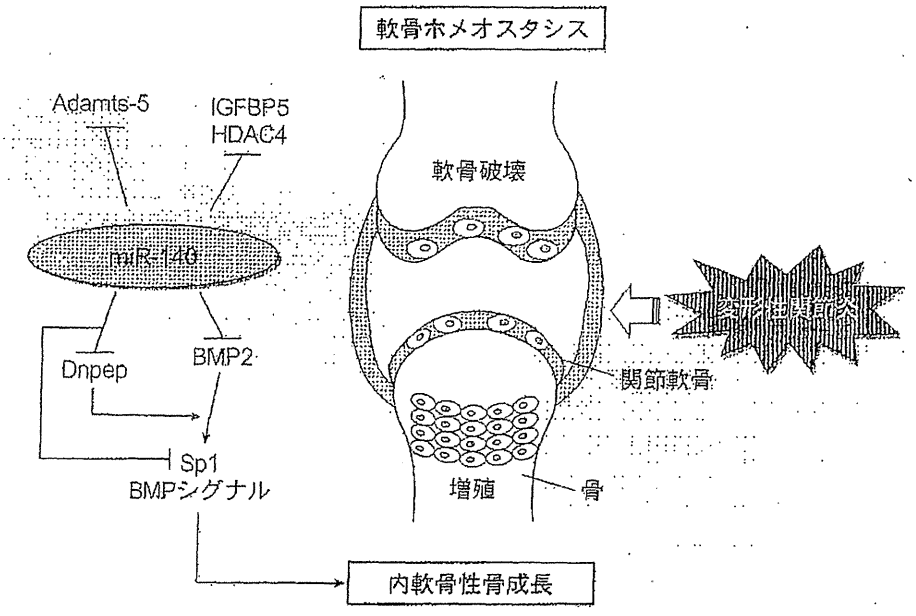

図　miR-140を介した軟骨発生・代謝制御機構

miR-140は，異なるターゲットを制御することで，内軟骨骨化と軟骨ホメオスタシスの両方を調節することができる。

BMP：bone morphogenetic protein，HDAC4：histone deacetylase 4，IGFBP5：insulin-like growth factor binding protein 5

（文献11より）

OA：osteoarthritis（変形性関節症），BMP：bone morphogenetic protein，AIA：antigen-induced arthritis
HDAC4：histone deacetylase 4（ヒストン脱アセチル化酵素4）
IGFBP5：insulin-like growth factor binding protein 5（インスリン様増殖因子結合タンパク質5）

低下，骨梁の減少なども起きており，OA軟骨におけるmiR-140の発現の低下が，BMPシグナルを介して軟骨下骨の変性にも関与していることが示唆される。これらの変性によるストレスの増加が，関節軟骨の変性を促進させOAの進行につながっているとする報告もある[14]。

軟骨ホメオスタシスにおけるmiR-140の役割を明らかにするため，時間軸でのmiR-140の変化を調べた結果，膝関節軟骨は生後1カ月まで正常であったが，3カ月以降は徐々にプロテオグリカンの減少や軟骨のフィブリレーションなどのOAの進行が確認された。また，サージカルOAモデルにおいても，miR-140ノックアウトマウスは術後8週でwild typeマウスと比べ有意にOAの進行が確認された。さらにmiR-140の軟骨変性への効果を調べるため，wild typeマウス，miR-140ノックアウトマウス，miR-140トランスジェニックマウスそれぞれの膝関節にantigen-induced arthritis (AIA) モデルを作製した結果，miR-140トランスジェニックマウスではプロテオグリカンとtype-Ⅱ collagenの減少に対する抵抗性が確認され，miR-140が炎症による軟骨変性に対して予防効果を持つことが示唆された[11]。miR-140が，OAの主要なプロテアーゼであるAdamts-5を直接の標的分子として抑制することがこの理由の一つであるが，軟骨細胞においてmiR-140によって抑制されると報告されているHDAC4 (histone deacetylase 4)，IGFBP5 (insulin-like growth factor binding protein 5) やBMPシグナルなどもこの結果の一因となっていると考えられる[10,12~14]。このようにmiR-140は，複数のpathwayにおいて多数の遺伝子をターゲットにしていることが明らかとなってきており，軟骨実質の生成や分解を調節し，軟骨のホメオスタシスを維持する主要なmiRNAであると言える。

おわりに

miR-140による軟骨治療は，早期のOAに対して理想的な治療薬となる可能性を秘めており，今後の研究が期待される。

文　献

1) Carthew RW, Sontheimer EJ：Origins and mechanisms of miRNAs and siRNAs. Cell 136：642-655, 2009.
2) Siomi H, Siomi MC：On the road to reading the RNA-interference code. Nature 457 (7228)：396-404, 2009.
3) Bernstein E, Kim SY, Carmell MA, et al：Dicer is essential for mouse development. Nat Genet 35：215-217, 2003.
4) Harfe BD, McManus MT, Mansfield JH, et al：The RNase Ⅲ enzyme Dicer is required for morphogenesis but not patterning of the vertebrate limb. Proc Natl Acad Sci U S A 102 (31)：10898-10903, 2005.
5) Kobayashi T, Lu J, Cobb BS, et al：Dicer-dependent pathways regulate chondrocyte proliferation and differentiation. Proc Natl Acad Sci U S A 105 (6)：1949-1954, 2008.
6) Wienholds E, Kloosterman WP, Miska E, et al：MicroRNA expression in zebrafish embryonic development. Science 309：310-311, 2005.
7) Ason B, Darnell DK, Wittbrodt B, et al：Differences in vertebrate microRNA expression. Proc Natl Acad Sci U S A 103：14385-14389, 2006.
8) Tuddenham L, Wheeler G, Ntounia-Fousara S, et al：The cartilage specific microRNA-140 targets histone deacetylase 4 in mouse cells. FEBS Lett 580：4214-4217, 2006.
9) Eberhart JK, He X, Swartz ME, et al：MicroRNA Mirn140 modulates Pdgf signaling during palatogenesis. Nat Genet 40：290-298, 2008.
10) Miyaki S, Nakasa T, Otski S, et al：MicroRNA-140 is expressed in differentiated human articular chondrocytes and modulates IL-1 re-

sponses. Arthritis Rheum 60 (9) : 2723-2730, 2009.
11) Miyaki S, Sato T, Inoue A, et al : MicroRNA-140 plays dual roles in both cartilage development and homeostasis. Genes Dev 24 : 1173-1185, 2010.
12) Nakamura Y, Inloes JB, Katagiri T, Kobayashi T : Chondrocyte-specific microRNA-140 regulates endochondral bone development and targets Dnpep to modulate bone morphogenetic protein signaling. Mol Cell Biol 31 : 3019-3028, 2011.
13) Yang J, Qin S, Yi C, et al : MiR-140 is co-expressed with Wwp2-C transcript and activated by Sox9 to target Sp1 in maintaining the chondrocyte proliferation. FEBS Lett 585 : 2992-2997, 2011.
14) Araldi E, Schipani E : MicroRNA-140 and the silencing of osteoarthritis. Genes Dev 24 : 1075-1080, 2010.